Materials Research. 2026; 29(suppl. 2): e20260142
DOI: https://doi.org/10.1590/1980-5373-MR-2026-0142

Development, Characterization and Application of Sustainable Ceramic Adsorbent Pellet for Textile Dye Removal

***Raphaela Ferraz Freitas*[a*], *Camila da Silva Rodrigues*[b], *Roberta Bueno Martins*[a], *Daniele Moreira*[a], *Agda Eunice de Souza*[a], *Marcela Prado Silva Parizi*[a], *Rosane Freire Boina*[a]**

[a]*Universidade Estadual Paulista (UNESP), Faculdade de Ciências e Tecnologia, Laboratório de Caracterização e Gestão de Resíduos Sólidos (LCGRS), Presidente Prudente, SP, Brasil.*
[b]*Universidade de São Paulo (USP), Escola Politécnica da USP, Departamento de Engenharia Química, Centro de Engenharia de Sistemas Químicos, Grupo de Pesquisa em Processos Oxidativos Avançados (AdOx), São Paulo, SP, Brasil.*

Received: April 29, 2026; Revised: August 04, 2026; Accepted: September 06, 2026

The textile industry is responsible for significant environmental impacts due to the generation of effluents that are difficult and costly to treat. Adsorption has emerged as an efficient and cost-effective technology for treating these effluents, particularly by utilizing waste materials, such as Water Treatment Plant Sludge (WTPS) and Yellow Passion Fruit Peel (YPP). This study aims to develop an adsorbent material from WTPS and YPP to remove the reactive blue dye BF5G from contaminated water. A ceramic adsorbent pellet (CAP) was produced, composed of 70% WTPS, 20% YPP, and 10% clay material, which was pressed and sintered at 210ºC. The CAP was characterized using XRF, XRD, FTIR, SEM, BET, and pH-PZC, and showed promise characteristics for use in adsorption. The CAP demonstrated a removal efficiency of 49.1%, with an adsorption capacity of 0.57 mg g^{-1} under optimal conditions of pH 3, 25ºC and a 120-minute stirring time.

Keywords: *Waste, Water Treatment Plant Sludge, Yellow Passion Fruit Peel, Adsorption, Blue Reactive Dye BF5G.*

1. Introduction

The textile industry is one of the primary sources of effluent, with significant potential for both qualitative and quantitative water contamination. These environmental impacts are particularly critical when effluents contain persistent and non-biodegradable compounds[1], such as reactive dyes. The textile dyeing sector accounts for approximately 20% of total industrial effluent discharges and ranks among the most polluting sectors globally[2]. In conventional garment manufacturing, polishing and dyeing processes alone require an average of 150 m^3 of water per ton of fabric produced[3]. Furthermore, it is estimated that about 15% of the dyes applied during textile processing are discharged into effluents[4,5].

Reactive dyes are complex, photochemically stable molecules that increase water turbidity, which reduces light penetration and consequently inhibits photosynthetic activity and causes toxic and carcinogenic effects to aquatic organisms[6]. Additionally, they contribute to increased organic load (biochemical oxygen demand - BOD), suspended solids, and concentrations of metal ions[7], as well as variations and instability in water pH[4]. Therefore, the treatment of textile industry effluents is necessary and challenging, leading researchers to develop cost-effective and efficient technologies that are technically and economically practical for large-scale applications.

Adsorption is a separation process that stands out in the treatment of contaminants due to its operational simplicity, selectivity, high removal efficiency[5], and the potential for simultaneous regeneration of the adsorbate, in accordance with the principles of the circular economy[5]. This surface phenomenon occurs through the interaction of physical and chemical forces and involves the accumulation of a specific substance at the surface or interface between two phases[7,8], where molecules of one substance accumulate on the surface of another. The adsorption process is influenced by the nature of the adsorbent and adsorbate and the operational parameters such as pH, temperature, pollutant concentration, contact time, and particle size of the adsorbent[7,8,9]. Determining characteristics of an effective adsorbent include high surface area, porosity, and the presence of functional groups or active sites for binding with the compound of interest[9,10].

Among adsorbent materials, various waste products generated in large amounts by society are reported to be promising for removing dyes, such as yellow passion fruit (*Passiflora edulis f. flavicarpa*) peel (YPP)[11-13] and water treatment plant sludge (WTPS)[4,14,15]. The biomass of YPP contains large amounts of pectin, cellulose, hemicellulose and other polysaccharides capable of removing a wide range of organic and inorganic pollutants[12], thus providing significant properties for the adsorption process. The WTPS

*e-mail: raphaela.freitas@unesp.br
Associate Editor: Luis Cabral.
Editor-in-Chief: Luiz Antonio Pessan.

is a by-product of water treatment processes constituted of aluminum, silica, iron, and various humic substances, which confer high reactivity and considerable pollutant removal capacity[16]. Table 1 presents a summary of the application of WTPS and YPP as adsorbent materials for the removal of pollutants such as metal ions, pharmaceuticals and, notably, textile dyes including methylene blue.

To render WTPS and YPP suitable as adsorbent materials, they are generally subjected to pretreatment, primarily thermal and chemical, using reagents such as H_3PO_4, $ZnCl_2$, $Ca(OH)_2$, $Fe(NO_3)_3$, HNO_3, NaOH, and H_2O_2. Adsorption experiments (Table 1) were conducted using adsorbent masses ranging from 0.01 to 1.0 g, pH values between 2 and 8, temperatures at 25ºC, initial pollutant concentrations from 0.1 to 200 $mg.L^{-1}$, and contact time between 30 to 3,360 minutes. Furthermore, both materials generally exhibited high removal efficiencies when applied individually, with an efficiency rate of 98.57%19 for WTPS in the removal of anti-inflammatory compounds and 99.86%[22] for yellow passion fruit peel in the removal of Cr (VI).

Despite the high efficiency, WTPS has a limited number of functional groups, which requires activation with chemicals or other substances[4,17,] to improve its kinetics and adsorption capacity. Among the possible waste-derived activators for WTPS, the peel of the yellow passion fruit stands out. The development of blends or composites to enhance the adsorption process is well established and frequently reported in the literature[23-26]. Furthermore, the production of adsorbent materials in pellet form is preferred over pulverized forms for industrial applications[27,28]. To date, the potential of a composite mixture of WTPS and YPP for dye removal via adsorption remains unexplored, representing a novel aspect of this study.

This study advances the development of adsorbent materials through the production and characterization of a ceramic adsorbent pellet (CAP), composed of WTPS and YPP, to remove reactive dyes from aqueous solutions. The adsorption experiments were carried out with the reactive blue dye BF5G. The CAP was produced to be simple to apply, durable, and in accord with sustainability principles, ensuring that the treated effluent complies with wastewater disposal regulations regarding reactive dye content.

2. Experimental

2.1. Preparation and production of Ceramic Adsorbent Pellet (CAP)

Fresh yellow passion fruits were acquired from a local market. The fruits were peeled, and the pulp was

Table 1. The use of Water Treatment Plant Sludge (WTPS) and Yellow Passion Fruit Peel (YPP) as an adsorbent for different types of pollutants.

Treatment	Ads*. amount (g)	Adb*.	C_0* ($mg.L^{-1}$)	pH	T* (ºC)	RE* (%)	q_e* ($mg.g^{-1}$)	t_e* (min)	Ref.*
Thermal, pulverization, chemical, with phosphoric acid (H_3PO_4) and encapsulation (PAS-AG and PAS-AR)	WTPS* (0.03)	Cd^{2+}	250	7	NR*	95	29.9	30	18
Pulverization, thermal and chemical with phosphoric acid (H_3PO_4)	WTPS (0.5)	Endocrine disruptors	0.1	5.5	25	NR	0.007	240	17
Thermal and chemical, with zinc chloride ($ZnCl_2$) and calcium hydroxide ($CaOH_2$)	WTPS (1.0)	Anti-inflammatory	30	8	25	98.57	217.28	120	19
Thermal and chemical, with iron nitrate ($Fe(NO_3)_3$)	WTPS (0.5)	Textile dyes (Anionic reactive blue 19 and methylene blue)	10	2-8	NR	35.55	NR	30	20
Pulverization and thermal	YPP* (1.0)	Textile dye (Methylene blue)	28.7	8	25	NR	NR	3360	21
Pulverization	YPP (0.01)	Textile dyes (Methylene blue and methyl violet)	50	8	25	NR	324.7 and 485.4	120	12
Pulverization, thermal and chemical with nitric acid (HNO_3)	YPP (0.1)	Textile dye (Eriochrome black)	100	6.8	25	NR	196	60	13
Spraying, thermal and chemical, with sodium hydroxide (NaOH) and hydrogen peroxide (H_2O_2)	YPP (1.0)	Cr (VI)	200	2	25	99.86	318	1440	22
Thermal treatment and pelletized	WTPS and YPP (~ 0.5)	Textile dye (Reactive blue dye)	30	3	25	71.57	0.540	240	This study

* Ads: Adsorbent; Adb: Adsorbate; C_0: initial adsorbate concentration ($mg{\cdot}L^{-1}$); T: temperature (°C); RE: removal efficiency (%); q_e: adsorption capacity at equilibrium time ($mg{\cdot}g^{-1}$); t_e: equilibrium time (min); WTPS: Water Treatment Plant Sludge; YPP: Yellow Passion Fruit Peel; NR: Not Reported; Ref: Reference.

removed. The YPP was thoroughly washed with distilled water, dried, and then oven-dried at 60ºC ± 3ºC to remove moisture. The dried material was milled using a cutting mill and subsequently sieved to obtain a fine particle size (<0.355 mm).

The sludge was supplied by a municipal water treatment plant (WTP) in the state of São Paulo, Brazil, which operates in a conventional cycle and uses Polyaluminum Chloride (PAC) as a coagulant and a non-ionic polyelectrolyte as a coagulation aid. The sludge was dewatered using a 105 $g \cdot m^{-2}$ non-woven geotextile blanket placed inside a high-density polyethylene (HDPE) box with a conical bottom, which was kept in a shaded area. The remaining moisture was removed by oven-drying at 100°C ± 3°C until a constant weight. The material was manually ground using a mortar and pestle, followed by mechanical milling in a plate mill and subsequent sieving through a 42-mesh Tyler sieve (<0.355 mm).

The plasticity was achieved by adding clay material (CM) collected from ceramics industries. The CM was oven-dried at 90ºC ± 3ºC for 24 hours, then milled using a plate mill and sieved through a 42-mesh Tyler sieve (<0.355 mm).

To produce the adsorbent, a mixture of precursor materials was prepared in the following proportions: 70% WTPS, 20% YPP, and 10% CM, consistent with the formulation reported by Mouratib et al.[29]. Approximately 0.5 g of the mixture was molded into a circular shape with a diameter of 13 mm and a thickness of 2 mm using a manual hydraulic press at 60 kN for 3 minutes. The resulting pellet was sintered in a muffle furnace at 210ºC (±5ºC)[30] to obtain the CAP. Figure 1 illustrates the process used to prepare the precursor materials WTPS, YPP, CM, and CAP.

2.2. Characterization of Yellow Passion Fruit Peel (YPP), Water Treatment Plant Sludge (WTPS), Clay Material (CM) and Ceramic Adsorbent Pellet (CAP)

The yellow passion fruit peel (YPP), dewatered and dried water treatment plant sludge (WTPS), and clay material (CM) were physicochemically characterized. The elemental composition was determined using X-ray fluorescence (XRF) analysis (Shimadzu, XRF-7000 spectrometer). The equipment can perform a scan ranging from Na to U, using a primary Rhodium (Rh) radiation source, focused on a 5 mm diameter collimator and a sample holder containing Mylar. The functional groups were evaluated by Fourier transform infrared spectroscopy (FTIR, Perkin Elmer Frontier IR). The analysis was carried out with a Perkin-Elmer Frontier IR spectrometer, operating at a spectral wavelength ranging from 200 to 2,000 cm^{-1} and a resolution of 0.5 cm^{-1}. Additionally, the crystallinity of the WTPS and CM, were determined for using X-ray diffraction (XRD), model XRD-6000, with Cu Kα radiation of $K\alpha_1$ = 1.5406 Å and $K\alpha_2$ = 1.5444 Å, at 40 kV and 30 mA current. The phases were identified using the Crystallographica Search-Match software (version 2.1), and the direct comparison method with the JCPDS-ICDD database (Joint Committee on Powder Diffraction Standards - International Centre for Diffraction Data). The morphology was examined by scanning electron microscopy (SEM). Each material was coated with a thin layer of gold and analyzed using a Carl Zeiss EVO LS15 microscope at magnification of 1,000× assess surface morphology and porosity.

The CAP was further characterized by X-ray fluorescence (XRF), Fourier transform infrared spectroscopy (FTIR), X-ray diffraction (XRD), and scanning electron microscopy (SEM). In addition, its surface properties were evaluated. The specific

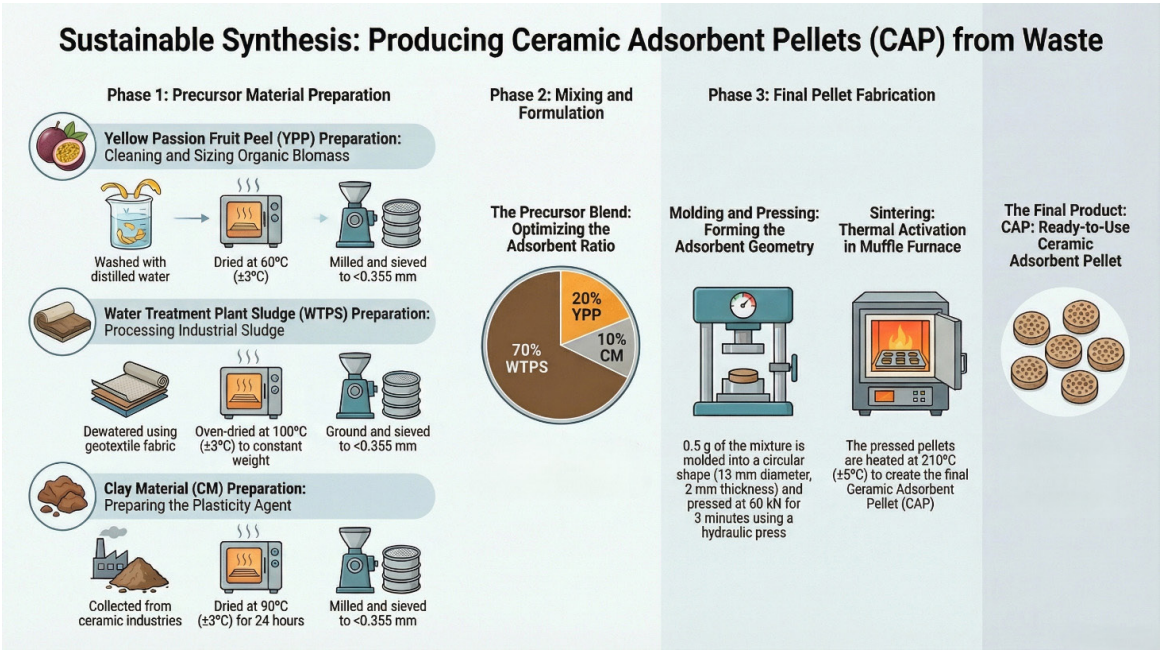


Figure 1. Process to produce the ceramic adsorbent pellet (CAP).

surface area, as well as pore volume and pore diameter, were determined through N_2 adsorption–desorption isotherms at -195.5°C using an ASAP 2020 Plus automated physisorption analyzer (Micromeritics, Norcross, GA), with calculations performed according to the Brunauer–Emmett–Teller (BET) method. The surface charge was evaluated by determining the point of zero charge (pH_pzc) according to the Point of Zero Charge (pH-PZC) method[31].

2.3. Batch Adsorption tests

The batch adsorption tests were performed in duplicate using CAP (~0.5 g) and 50 mL of aqueous solution containing reactive blue dye BF-5G at initial concentration 10 mg L^{-1}. The experiments were carried out in a shaker incubator (Lucadema, LUCA-222) at 120 rpm, with temperature controlled.

The synthetic solutions before and after treatment were analyzed using a UV-Vis spectrophotometer at 621 nm, and the dye concentration was determined according to the previously established calibration curve. The adsorption capacity (q), or adsorption rate, and the removal efficiency (ER) were calculated using Equation 1 and Equation 2, respectively.

$$q\left(mg.g^{-1}\right)=\frac{\left(C_0-C_e\right)}{m}.V \quad (1)$$

$$ER(\%)=\frac{\left(C_0-C_f\right)}{C_0}.100 \quad (2)$$

Where: C_0 is the initial solute concentration (mg L^{-1}); C_e is the equilibrium solute concentration (mg L^{-1}); C_f is the final concentration after treatment (mg L^{-1}); V is the solution volume (L); m is the mass of the dry adsorbent (g).

To evaluate the potential release of undesirable compounds from the CAP (~0.5 g) during the treatment process, a blank experiment was conducted using 50 mL of distilled water at pH 7 and 25 °C, with contact times of 2, 4, and 6 h.

The adsorption capacity, as well as the removal efficiency obtained, allows the determination of the most favorable conditions for the treatment of BF5G dye in aqueous solution in terms of pH, adsorbent dosage, temperature and contact time. The effect of solution pH was investigated by adjusting the pH to 3, 8, and 10. The experiments were conducted at 25°C using one CAP (~0.5 g) with a contact time of 24 h. The pH conditions that yielded the highest adsorption capacity and removal efficiency were selected for subsequent experiments. Subsequently, the effect of temperature was evaluated through adsorption experiments conducted at 25, 35, and 45°C, while maintaining constant adsorbent dosage (~0.5 g), pH, and contact time (24 h). The effect of adsorbent dosage was then investigated over a range of 1 to 3 units (corresponding to approximately 0.5 - 1.5 g of CAP), with pH, temperature (25°C), and contact time (24 h) kept constant. Thereafter, the effect of contact time was assessed by performing adsorption experiments at 2, 4, 6, and 24 h, 25°C, pH fixed, and using one CAP (~0.5 g).

An extended study under optimal experimental conditions was conducted using dye solutions with concentrations of 5, 10, 15, 20, 25, and 30 mg·L^{-1} to evaluate the adsorption performance.

3. Results and Discussion

3.1. Chemical and mineralogical composition of precursor residues and ceramic pellet

The chemical composition analysis (Table 2) revealed that the predominant elements in WTPS, CM and CAP are silica oxide (~50%), aluminum (~30%) and iron (~9%). These constituents may contribute to the thermal and chemical stability of CAP. In WTPS, the presence of aluminum and iron is attributed to the use of coagulant agents based on these elements during the water treatment process[15]. Furthermore, WTPS and CM exhibit similar mineralogical characteristics[32], resulting in the occurrence of common phases in both materials, such as aluminum and iron oxides and hydroxides[33].

The YPP is composed mainly of potassium (64%), calcium (17%) and silicon (6%), which is associated with the natural composition of the biomass[34]. Nayeri and Mousavi (2020) reported that potassium oxide compounds can enhance the thermal degradation resistance of a material[35].

Thus, CAP contains compounds derived from precursor materials, such as silicon, aluminum, iron, potassium and titanium oxides, which have been shown to be capable of adsorbing pollutants in aqueous solution[36,37].

Regarding the crystalline structure of the precursor materials and the pellets (Figure 2), the phases of illite (I), quartz (Q), and calcite (C) were identified in WTPS and CM. The mineralogical composition of CAP revealed a predominance of crystalline structures corresponding to quartz. Quezada *et al*. (2022) emphasize that the presence of quartz in CAP is advantageous for the adsorption mechanism[38]. YPP did not exhibit crystalline phases.

Figure 3 shows the identification of functional groups in the precursor materials (WTPS, YPP, and CM) and in CAP. WTPS and CM exhibit similar transmittance bands corresponding to: the stretching of OH and NH groups (3,822, 2,977 e 2,790 cm^{-1}); the presence of carbon (1,505, 1,489 e 1,218 cm^{-1}) and the Si-O-Si and Si-O-Al groups, due

Table 2. Chemical composition (in wt%) of the water treatment plant sludge (WTPS), clay material (CM), yellow passion fruit peel (YPP) and ceramic adsorbent pellet (CAP).

Composition (%)	SiO_2	Al_2O_3	Fe_2O_3	TiO_2	K_2O	CaO	SO_3	P_2O_5	Others
WTPS	50.09	33.35	10.75	2.09	1.58	-	-	-	2.14
CM	55.67	27.81	9.85	1.39	3.80	-	-	-	1.48
YPP	6.30	-	2.20	-	64.66	17.38	4.92	2.82	1.71
CAP	51.49	33.14	9.34	1.8	2.24	-	-	-	1.99

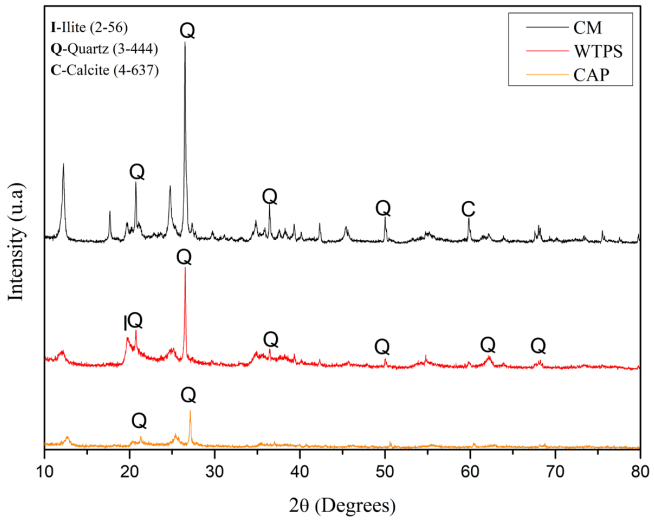


Figure 2. X-ray diffraction (XRD) pattern of the water treatment plant sludge (WTPS), clay material (CM), and ceramic adsorbent pellet (CAP).

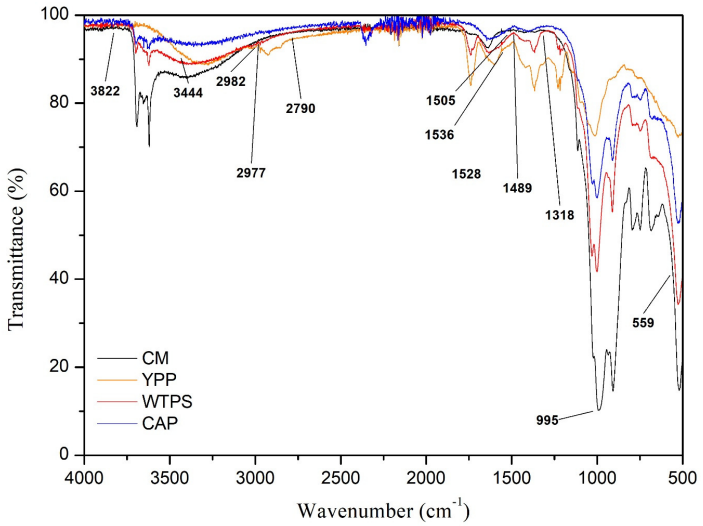


Figure 3. FTIR spectra of the precursor materials: water treatment plant sludge (WTPS), yellow passion fruit peel (YPP), clay material (CM), and ceramic adsorbent pellet (CAP).

to the deformation of the structural hydroxyl group (995 e 559 cm^{-1})[39,40]. For YPP, transmittance bands were observed at 3,444, 2,982, 2,234, 1,536 cm^{-1}, representing the stretching of C=O, C-O, C=C[41], which indicate the presence of compounds derived from pectin and cellulose. The presence of these groups is associated with a high capacity for pollutant adsorption[22,42-44] CAP retains characteristics of its precursors, indicating the presence of active sites capable of adsorbing pollutants, which is desirable for the present study.

3.2. Morphology, area and surface charge of precursors and Ceramic Adsorbent Pellet (CAP)

Figure 4 (a-c) shows the morphology of WTPS, YPP and CAP at magnification of 1,000x. WTPS exhibits a rough structure with some overlapping grains, a morphology consistent with that reported by Martins et al.[18]. YPP displays an irregular surface with particles of different sizes and

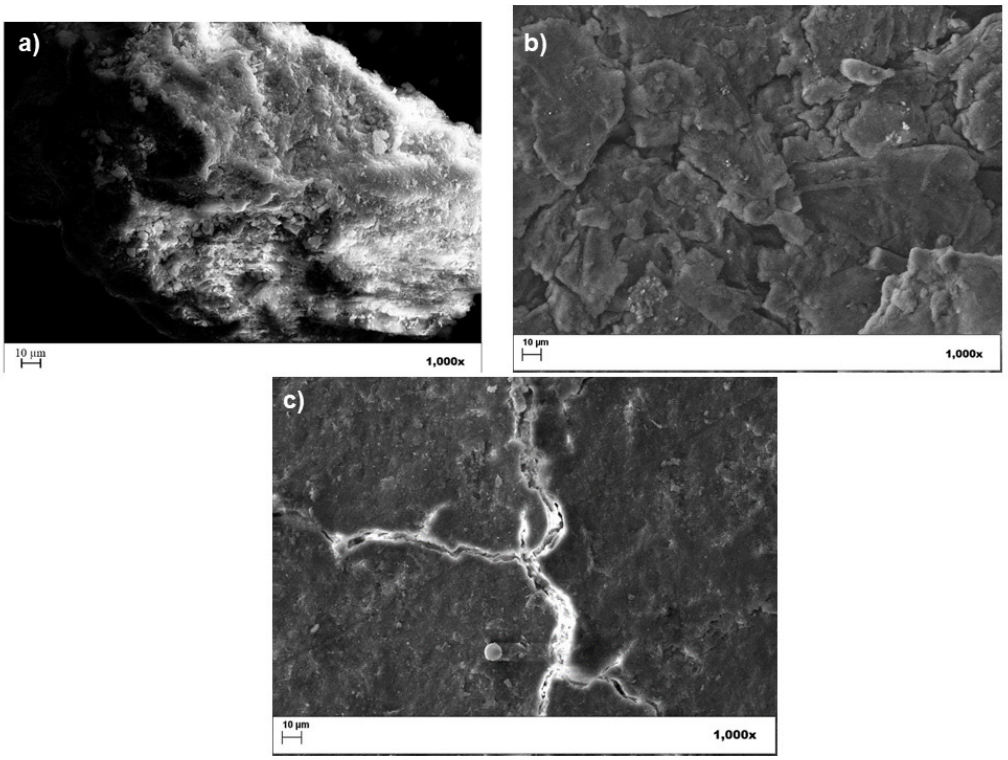


Figure 4. Scanning Electron Microscopy (SEM) images of WTPS (a), YPP (b), and CAP (c) at 1,000x.

well-defined grains, in addition to the absence of pores, similar to that reported by Yu et al.[45]. Furthermore, Ramos et al.[46] explain that the differences in grain size can be attributed to the distinct thicknesses and rigidity of passion fruit peel structures. CAP, in turn, presents a smooth structure with deep fissures and grains very similar to those found in passion fruit peel. According to Boina et al.[16], rough and porous materials generally provide a larger surface area, enhancing the interaction between adsorbate and adsorbent.

For a material to be considered a good adsorbent, it is important to evaluate its properties, especially its specific surface area[47]. Materials with higher surface areas tend to provide more active sites, which may favor an increase in adsorption capacity[48]. Therefore, the textural properties of CAP (Table 3) indicate that its surface area is mainly composed of mesopores, accounting for more than 65% of the total surface area, with a pore diameter of 6.255 nm. The pore volume of the material is 0.064 $cm^3\ g^{-1}$. In addition, the surface area of CAP (41.251 $m^2\ g^{-1}$) is considered small when compared to that of activated carbons (500 $m^2\ g^{-1}$)[48], however, products derived from agro-industrial residues tend to exhibit lower surface areas[49]. Studies conducted with biosorbents based on pine nut shell[50], papaya seeds[51], and passion fruit peel[42] resulted in surface areas of 63.00, 1.38, and 30.0 $m^2\ g^{-1}$, respectively.

Regarding the surface charge (Table 3), the pH at the point of zero charge (pH-PZC) of the adsorbent material was determined to be 7.955. When the pH of a solution is higher than the pH-PZC, the material becomes negatively charged, favoring the adsorption of cations. Conversely, at pH values below the pH-PZC, the adsorption of anions is facilitated[52]. Considering the anionic nature of the reactive blue dye[53], adsorption at pH values below 7.955 will be favored, as CAP will be positively charged.

3.3. Blank experiment

Interference associated with color release from CAP resulted in an absorbance peak (Figure 5) at approximately 290 nm. This phenomenon is likely attributed to the presence of carotenoids[54] in the YPP composition and is further intensified when the CAP dosage exceeds one pellet (~0.5 g). It should be emphasized that at 621 nm no release of compounds into water occurred that could influence the observed results.

3.4. Adsorption assays

In the evaluation of adsorption capacity regarding the effect of pH (Figure 6), pH 3 achieved the highest adsorption capacity (0.431 mg g^{-1}) and a removal efficiency of approximately 46%. This is due to the anionic nature of the studied dye, whose surface is positively charged under acidic pH conditions, favoring the adsorption process[55]. Under other pH conditions (pH 8 and 10), the removal effect was lower than 10%. Other studies investigating dye adsorption have reported similar results to those obtained in this work, in which alkaline conditions, especially at pH 8 and 10, led to a decrease in pollutant removal efficiency and, consequently, in adsorption capacity[16,56,57]. This behavior may be related to the dissociation constants of the pollutant (pKa_1 = 4.602 and pKa_2 = 7.031), since changes in pH can alter its ionization state and, consequently, its interaction with the adsorbent surface[16,58].

Table 3. Surface characteristics of the ceramic absorbent pellet (CAP) regarding specific surface area (S_{BET}), pore volume (V_p), pore diameter (d_p), and pH at the point of zero charge (pH-PZC).

CAP	S_{BET} ($m^2.g^{-1}$)	V_p ($cm^3.g^{-1}$)	d_p (nm)	pH-PCZ
	41.251±1.158	0.064	6.255	7.955±2.271

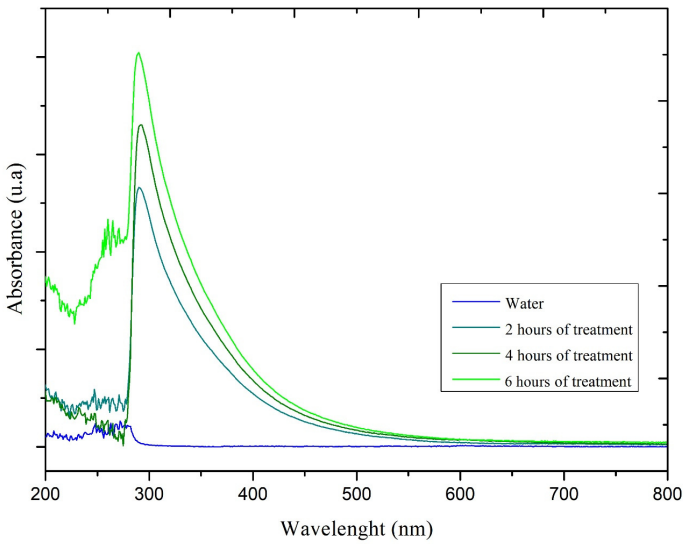


Figure 5. Absorption spectrum of CAP (~0.5 g) in distilled water at different contact times. The assay was conducted with 100 mL of solution at 25ºC and pH 7.

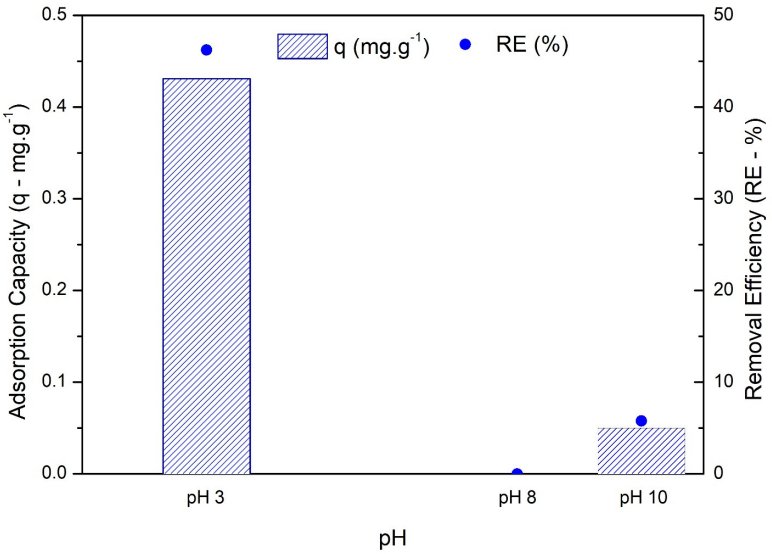


Figure 6. Calculated adsorption capacity (q_e, $mg.g^{-1}$) and removal efficiency (RE, %) as a function of pH variation. The assay was conducted using a 10 $mg.L^{-1}$ solution at 25ºC, with a contact time of 24 h and one pellet mass (~0,5 g).

It is noteworthy that during the adsorption process, under mechanical stirring at 120 rpm, CAP deformation occurred, causing particle detachment, which contributed to an increase in the solution turbidity and, consequently, interfered with the measurement of the final concentration. The same effect was observed in all tests.

In the analysis of temperature variation during the treatment (Figure 7), at 45ºC the calculated adsorption capacity was

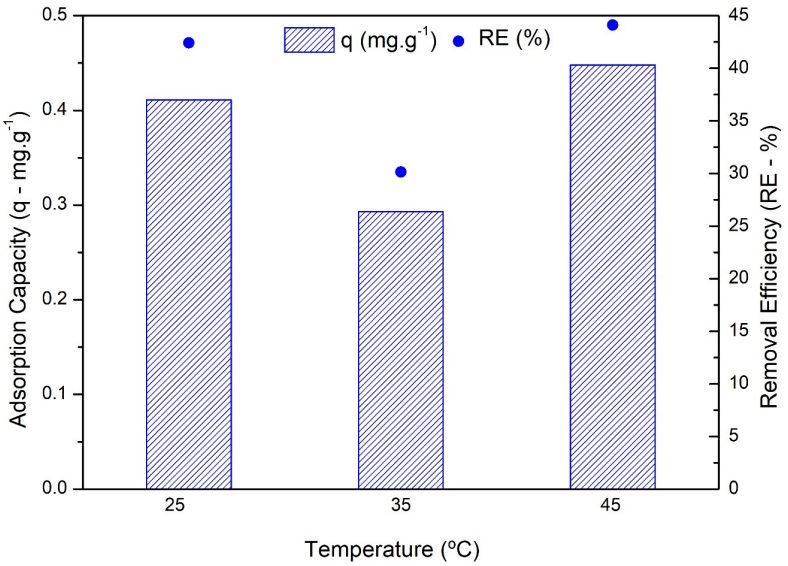


Figure 7. Adsorption capacity (q, mg.g^{-1}) and removal efficiency (RE, %) at different temperatures. The assay was conducted using a 10 mg L^{-1} solution at pH 3, with a contact time of 24 h, and one pellet mass (~0,5 g).

0.448 mg g^{-1}, with a dye removal efficiency of 44% in the aqueous solution. Similar results were also obtained at 25ºC, with an adsorption capacity of 0.411 mg g^{-1} and a removal efficiency of 42.41%. The increase in temperature favors the adsorption process, as it accelerates the diffusion of molecules in solution to the adsorbent surface, increasing the kinetic energy of the molecules and the adsorption rate[59]. In addition, the increase in temperature enhances the ionization of available functional groups, making them more active in the adsorption process[60]. Given the minimal variation in treatment efficiency (<4%), and considering process cost-effectiveness for industrial applications, 25°C was selected for all subsequent experiments.

Regarding the effect of the amount of CAP used in the adsorption process (mass effect) on the removal of reactive blue dye, the test with approximately 0.5 g of CAP resulted in an adsorption capacity of 0.288 mg g^{-1} and a removal efficiency of 29.51% (Table 4). For the remaining experiments, final concentrations were higher than the initial ones, indicating the presence of interferences in the analysis, which resulted in a null effect on the calculation of adsorption capacity. Thus, the use of a single pellet was effective for the proposed treatment and was adopted for the subsequent tests.

In terms of contact time (Table 5), satisfactory results were obtained for the tests at 120, 240, and 720 minutes, with efficiencies of 41.24%, 45.14%, and 45.98% and adsorption rates of 0.41, 0.43, and 0.46 mg g^{-1}, indicating a rapid process. The test performed at 1440 minutes showed a lower adsorption capacity (0.225 mg g^{-1}) and, consequently, a lower efficiency (23.37%). The high adsorption capacity and removal efficiency observed at the initial times are associated with the high availability of active sites, which gradually become saturated[61]. Over time, the remaining sites become less accessible due to repulsive forces between solute molecules on the adsorbent surface and in solution[62].

Figure 8 illustrates the result of the FTIR analysis of the pellet before and after the adsorption tests. The analysis confirmed the occurrence of adsorption and involvement of active functional groups in the process, as evidenced by the band at 667 cm^{-1}, which indicates bending and stretching of the OH and N-H groups present in the reactive blue dye[63,64].

3.5. Extended adsorption study

For the other concentration ranges of reactive blue dye in solution (Figure 9), the treatment achieved a removal efficiency above 40%, with the adsorption capacity of CAP increasing as the dye concentration in the synthetic effluent rose.

The maximum adsorption capacity (0.57 mg.g^{-1}) was reached at 120 minutes (2 hours) using an initial concentration of 30 mg L^{-1} of BF-5G, whereas a concentration of 5 mg L^{-1} resulted in a value six times lower. These results suggest that the process is highly dependent on the adsorbate concentration and is limited by the number of active sites available on the adsorbent surface. Similar behaviors have been reported in other studies using passion fruit peel for dye adsorption[21], which achieved removal efficiencies of approximately 84.2% and 90%, and adsorption rates of 1.995 mg g^{-1} and 0.006 mmol g^{-1}, respectively.

The UV-Vis spectra after the treatments (Figure 10) showed lower absorbance at 621 nm compared to the raw effluent (before treatment), indicating the effective removal of reactive blue dye in all tests.

However, the release of chromophore compounds from CAP was observed at 290 nm. This finding underscores the need for YPP pre-treatment prior to pellet formation

Table 4. Results of the preliminary adsorption study using different amounts of CAP (mass effect). Calculated adsorption capacity (q_e, $mg.g^{-1}$) and removal efficiency (RE, %) as a function of the amount of CAP. The assay was conducted using 10 mg L^{-1} solution at 25ºC, pH 3, and a contact time of 24 h.

CAP (Unit)	qc ($mg.g^{-1}$)	RE (%)
1	0.288	29.51
2	NC	NC
3	NC	NC

Table 5. Effect of contact time (120, 240, 720 e 1440 minutes) on the adsorption capacity and removal efficiency of the reactive blue dye (10 mg L^{-1}) using CAP (~ 0,5 g). The assay was conducted at 25ºC and pH 3.

Contact time (minutes)	qc ($mg.g^{-1}$)	RE (%)
120	0.414	41.243
240	0.430	45.139
720	0.457	45.986
1440	0.225	23.374

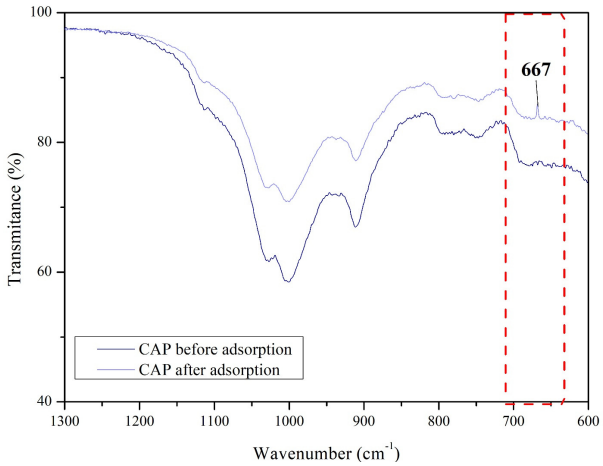


Figure 8. FTIR spectra of the ceramic absorbent pellet (CAP) before and after the preliminary adsorption tests. The analysis was performed using the pellet employed in the treatment with a 10 $mg.L^{-1}$ reactive blue dye solution at pH 3 and 25ºC for 24 h.

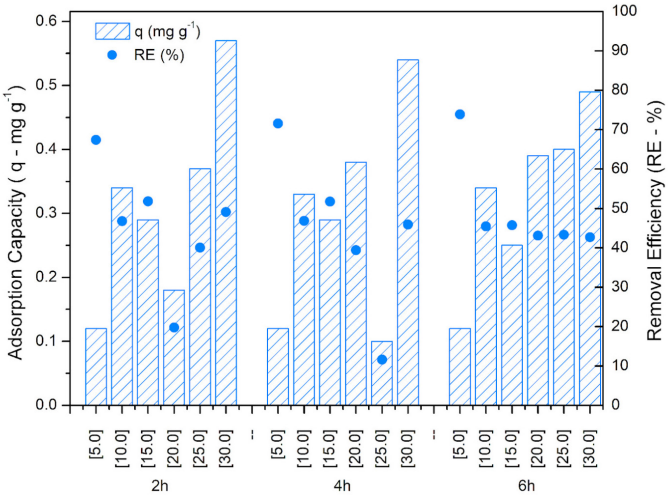


Figure 9. Adsorption capacity (q, $mg.g^{-1}$) and removal efficiency (RE, %) for solution of reactive dye concentrations of 5, 10, 15, 20, 25, and 30 mg L^{-1}. The assay was conducted at pH 3, with 100 mL, at 25ºC, using one CAP (~0,5 g), and varying contact time (Tc).

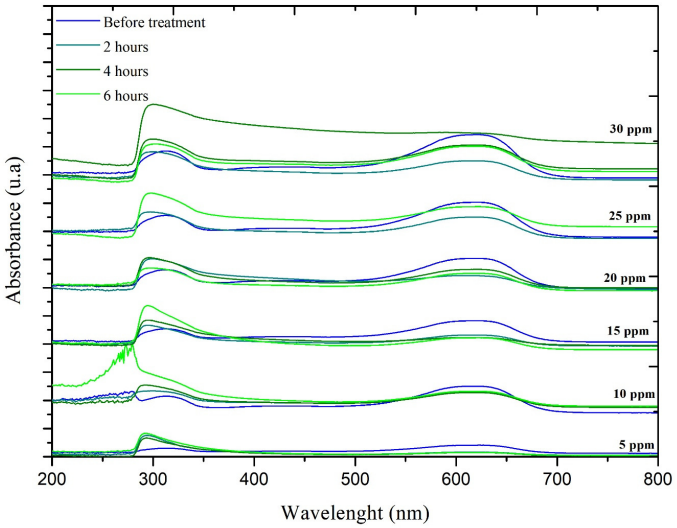


Figure 10. Absorption curve of the Reactive Blue BF-5G dye at concentrations of 5, 10, 15, 20, 25, and 30 mg.L^{-1} before and after adsorption at different contact times (2, 4, and 6 h). The assay was conducted with 50 mL of solution, one CAP (~0.5 g), at 25°C and pH 3.

or enhanced thermal activation of CAP to promote the removal of carotenoids while preserving the functional groups responsible for adsorption. Under those conditions, the proposed treatment would comply with discharge requirements for water bodies, ensuring the absence of both toxic substances and the virtually present materials.

4. Conclusions

The activation process of WTPS with YPP for the production of CAP proved to be effective, increasing porosity and incorporating the functional groups of interest, thereby enhancing the dye retention capacity. CAP exhibited a BET surface area of 41.25 m^2 g^{-1} and a point of zero charge at pH 7.9. The adsorption study demonstrated the material's effectiveness in removing reactive blue dye (BF-5G), achieving a maximum removal efficiency of 49.1% and a maximum adsorption capacity of 0.57 mg g^{-1} over a two-hour treatment period. The optimal treatment conditions included pH 3, a temperature of 25ºC, a pellet mass of 0.5 g and a stirring time of 120 minutes at 120 rpm. Further studies are recommended to elucidate the mechanisms involved in this process, explore the application of the pellets for other pollutants and improve the understanding of dye release during adsorption treatment.

5. Acknowledgments

The authors gratefully acknowledge the financial support from The São Paulo Research Foundation (FAPESP - Process number 2022/16242-2).

6. Data Availability

All data supporting the findings of this study are provided in the article itself.

7. References

1. Maurya NS, Mittal AK, Cornel P, Rother E. Biosorption of dyes using dead macro fungi: effect of dye structure, ionic strength and pH. Bioresour Technol. 2006;97(3):512-21. https://doi.org/10.1016/j.biortech.2005.02.045. PMid:16216733.
2. Tariq MF, Javed F, Ikhlaq A, Qazi UY, Mahmood K, Javaid R. Application of In-situ electrocoagulation/ZIF 67@ZIF 8 catalytic ozonation followed by ceramic membrane filtration process for textile wastewater remediation. Colloids and Surfaces A. Colloids Surf A Physicochem Eng Asp. 2026;731:139044. https://doi.org/10.1016/j.colsurfa.2025.139044.
3. Samsami S, Mohamadizaniani M, Sarrafzadeh M-H, Rene ER, Firoozbahr M. Recent advances in the treatment of dye – containing wastewater from textile industries: overview and perspectives. Process Saf Environ Prot. 2020;143:138-63. https://doi.org/10.1016/j.psep.2020.05.034.
4. Kaykhaii M, Sasani M, Marghzari S. Removal of dyes from the environment by adsorption process. Chemical and Materials Engineering. 2018;6(2):31-5. https://doi.org/10.13189/cme.2018.060201.
5. Qu J. Research progress of novel adsorption processes in water purification: A review. J Environ Sci (China). 2008;20(1):1-13. https://doi.org/10.1016/S1001-0742(08)60001-7. PMid:18572516.
6. Ali I, Gupta VK. Advances in water treatment by adsorption technology. Nat Protoc. 2007;1(6):2661-7. https://doi.org/10.1038/nprot.2006.370. PMid:17406522.
7. Do Nascimento RF, De Lima ACA, Vidal CB, Melo D. Q., Raulino GSC. Adsorção: aspectos teóricos e aplicações ambientais. Fortaleza: Imprensa Universitária; 2014.
8. Akhtar M, Sarfraz M, Ahmad M, Raza N, Zhang L. Use of low-cost adsorbent for waste water treatment: recent progress, new trend and future perspectives. Desalination Water Treat. 2025;321:100914. https://doi.org/10.1016/j.dwt.2024.100914.
9. Saĝlam S, Türk FN, Arslanoĝlu H. Use and applications of metal-organic frameworks (MOF) in dye adsorption: review. J Environ Chem Eng. 2023;11(5):110568. https://doi.org/10.1016/j.jece.2023.110568.
10. Goswami D, Mukherjee J, Mondal C, Bhunia B. Bioremediation of azo dye: a review on strategies, toxicity assessment, mechanisms, bottlenecks and prospects. Sci Total Environ. 2024;954:176426. https://doi.org/10.1016/j.scitotenv.2024.176426. PMid:39326754.

11. Lima EC, Royer B, Vaghetti JC, Simon NM, da Cunha BM, Pavan FA, et al. Application of Brazilian pine - fruit shell as a biosorbent to removal of reactive red 194 textile dye from aqueous solution: kinetics and equilibrium study. J Hazard Mater. 2008;155(3):536-50. https://doi.org/10.1016/j.jhazmat.2007.11.101. PMid:18178307.
12. Lin H, Chen K, Du L, Gao P, Zheng J, Liu Y, et al. Efficient and selective adsorption of methylene blue and methyl violet dyes by yellow passion fruit peel. Environ Technol. 2021;43(23):3519-30. https://doi.org/10.1080/09593330.2021.1924288. PMid:33944677.
13. Brito SMO, Cordeiro JLC, Ramalho LC, Oliveira JFR. Eriochrome black adsorption on yellow passion fruit peel (Passiflora edulis f. Flavicarpa) treated with sodium hydroxide and nitric acid: study of adsorption isotherms kinetic models and thermodynamic parameters. SN Appl Sci. 2019;1:1226. https://doi.org/10.1007/s42452-019-1266-x.
14. Gadekar MR, Ahammed MM. Removal of disperse dye from aqueous solution in fixed-bed column by water treatment residuals. Desalination Water Treat. 2018;102:264-72. https://doi.org/10.5004/dwt.2018.21840.
15. Pieczykolan B, Krzyżowska P. Removal of Helaktyn Blue F-2R via adsorption onto modified post-coagulation sludge. Desalination Water Treat. 2022;275:103-15. https://doi.org/10.5004/dwt.2022.28802.
16. Boina RF, Estevam BR, Freitas RF, Rodrigues JMM, Boina WLO, Sales DH, et al. Ceramic adsorbent material in removing reactive blue bf 5G dye from synthetic wastewater. Separ Purif Tech. 2024;331:125555. https://doi.org/10.1016/j.seppur.2023.125555.
17. Siswoyo E, Mihara Y, Tanaka S. Determination of key components and adsorption capacity of a low-cost adsorbent based on sludge of drinking water treatment plant to adsorb cadmium ion in water. Appl Clay Sci. 2014;97-98:146-52. https://doi.org/10.1016/j.clay.2014.05.024.
18. Martins DS, Estevam BR, Perez ID, Américo-Pinheiro JHP, Isique WD, Boina RF. Sludge from a water treatment plant as an adsorbent of endocrine disruptors. J Environ Chem Eng. 2022;4(4):108090. https://doi.org/10.1016/j.jece.2022.108090.
19. Siswoyo E, Qoniah I, Lestari P, Fajri JA, Sani RA, Sari DG, et al. Development of a floating adsorbent for cadmium derived from modified drinking water treatment plant sludge. Environ Technol Innov. 2019;14:100312. https://doi.org/10.1016/j.eti.2019.01.006.
20. Valério Filho A, Tholozan LV, Arim AL, De Almeida ARF, Da Rosa GS. High-performance removal of anti-inflammatory using activated carbon from water treatment plant sludge: fixed-bed and batch studies. Int J Environ Sci Technol. 2023;20(4):3633-44. https://doi.org/10.1007/s13762-022-04215-7.
21. Laib S, Rezzaz-Yazid H, Sadaoui Z. Comparative study on removal of textile dyes in aqueous medium by adsorption using modified drinking water treatment sludge. Arab J Sci Eng. 2022;47(5):6085-98. https://doi.org/10.1007/s13369-021-05950-8.
22. Pavan FA, Mazzocato AC, Gushikem Y. Removal of methylene blue dye from aqueous solutions by adsorption using yellow passion fruit peel as adsorbent. Bioresour Technol. 2008;99(8):3162-5. https://doi.org/10.1016/j.biortech.2007.05.067. PMid:17692516.
23. Zhao X, Zheng J, You S, Du L, Liu C, Chen K, et al. Selective adsorption of Cr (VI) onto amine-modified passion fruit peel biosorbent. Processes (Basel). 2021;9(5):790. https://doi.org/10.3390/pr9050790.
24. Sun B, Ge X, Zhou H, Guo Y, Wang Y, Bao L, et al. Efficient removal of tetracycline from water using copper MOFs/bismuth molybdate composite nano adsorbent. Desalination Water Treat. 2024;320:100589. https://doi.org/10.1016/j.dwt.2024.100589.
25. Neeti K, Singh R, Ahmad S. Adsorptive removal of fluoride uptake from aqueous media using novel composite adsorbent. Environ Pollut Manag. 2024;1:49-61. https://doi.org/10.1016/j.epm.2024.03.001.
26. Li H, Zhu X, Zhao J, Ling G, Zhang P. Emerging adsorbents: applications of sodium alginate/graphene oxide composite materials in wastewater treatment. J Water Process Eng. 2024;59:105100. https://doi.org/10.1016/j.jwpe.2024.105100.
27. Santos DC, Adebayo MA, Lima EC, Pereira SFP, Cataluña R, Saucier C, et al. Application of carbon composite adsorbents prepared from coffee waste and clay for the removal of reactive dyes from aqueous solutions. J Braz Chem Soc. 2015;26:924-38. https://doi.org/10.5935/0103-5053.20150053.
28. Kang S, Choi JW, Park JG, Baek K. Pellet adsorbent derived from molasses and dewatered alum sludge for arsenic removal. J CO2 Util. 2019;33:31-6. https://doi.org/10.1016/j.jcou.2019.05.002.
29. Mouratib R, Achiou B, El Krati M, Younssi SA, Tahiri S. Low-cost ceramic membrane made from alumina and silica-rich water treatment sludge and its application to wastewater filtration. J Eur Ceram Soc. 2020;40(15):5942-50. https://doi.org/10.1016/j.jeurceramsoc.2020.07.050.
30. Ramos BP, Perez ID, Paiano MS, Vieira MGA, Boina RF. Activated carbons from passion fruit shells in adsorption of multimetal wastewater. Environ Sci Pollut Res. 2021;29(1):1446-57. https://doi.org/10.1007/s11356-021-15449-2.
31. Regalbuto JR, Robles JO. The engineering of Pt/carbon catalyst preparation for application on proton exchange fuel cell membrane (PEFCM). Chicago: Catalysis Laboratory, University of Illinois at Chicago; 2004.
32. Hegazy BE-DE, Fouad HA, Hassanain AM. Incorporation of water sludge, silica fume, and rice husk ash in brick making. Adv Environ Res. 2012;1(1):83-96. https://doi.org/10.12989/aer.2012.1.1.083.
33. Teixeira SR, Santos GTA, Souza AE, Alessio P, Souza SA, Souza NR. The effect of incorporation of a Brazilian water treatment plant sludge on the properties of ceramic materials. Appl Clay Sci. 2011;53(4):561-5. https://doi.org/10.1016/j.clay.2011.05.004.
34. Peres CP, de Morais LC, Resende PMR. Carbon adsorption on waste biomass of passion fruit peel: a promising machine learning model for CO2 capture. J CO2 Util. 2024;80:102680. https://doi.org/10.1016/j.jcou.2024.102680.
35. Nayeri D, Mousavi SA. Dye removal from water and wastewater by nanosized metal oxides - modified activated carbon: a review on recent researches. J Environ Health Sci Eng. 2020;18(2):1671-89. https://doi.org/10.1007/s40201-020-00566-w. PMid:33312670.
36. Shafizah IN, Irmawati R, Omar H, Yahaya M, Aina AA. Removal of free fatty acid (FFA) in crude palm oil (CPO) using potassium oxide/dolomite as an adsorbent: Optimization by Taguchi method. Food Chem. 2022;373(Pt B):131668. https://doi.org/10.1016/j.foodchem.2021.131668.
37. Choi J, Chung J, Lee W, Kim J-O. Phosphorus adsorption on synthesized magnetite in wastewater. J Ind Eng Chem. 2016;34:198-203. https://doi.org/10.1016/j.jiec.2015.11.008.
38. Quezada GR, Mejía A, Piceros E, Robles P, Nieto S, Gálvez E, et al. Describing the adsorption of sodium tripolyphosphate on kaolinite surfaces in a saline medium by molecular dynamics. Miner Eng. 2022;175:107280. https://doi.org/10.1016/j.mineng.2021.107280.
39. Machado MCP, Langbehn JT, Oliveira CM, Elyseu F, Cargnin M, Júnior De Noni A, et al. Estudo do comportamento e caracterizações de argilas bentoníticas após processo de liofilização. Ceramica. 2018;64(370):207-13. https://doi.org/10.1590/0366-69132018643702324.
40. Oliveira SMAC. Análise de desempenho e confiabilidade de estações de tratamento de esgotos [tese]. Belo Horizonte: Escola de Engenharia, Universidade Federal de Minas Gerais; 2006 [cited 2025 Jan 28]. Available from: https://repositorio.ufmg.br/bitstream/1843/ENGD-6RFQ6F/1/silviamaria21.pdf
41. Macedo MCC, Correia VTV, Silva VDM, Pereira DTV, Augusti R, Melo JOF, et al. Development and characterization of Yellow Passion Fruit Peel Flour (Passiflora edulis f. flavicarpa). Metabolites.

2023;13(6):684. https://doi.org/10.3390/metabo13060684. PMid:37367845.
42. Pavan FA, Lima EC, Dias SLP, Mazzocato AC. Methylene blue biosorption from aqueous solutions by yellow passion fruit waste. J Hazard Mater. 2008;150(3):703-12. https://doi.org/10.1016/j.jhazmat.2007.05.023. PMid:17597293.
43. De Oliveira FM, Coelho LM, De Melo EI. Avaliação de processo adsortivo utilizando mesocarpo de coco verde para remoção do corante azul de metileno. Materia (Rio J). 2018;23(4):e-12223. https://doi.org/10.1590/s1517-707620180004.0557.
44. Banerjee S, Chattopadhyaya MC. Adsorption characteristics for the removal of a toxic dye, tartrazine from aqueous solutions by a low cost agricultural by-product. Arab J Chem. 2017;10:S1629-38. https://doi.org/10.1016/j.arabjc.2013.06.005.
45. Yu S, Yan J-K, Jin M-Y, Li L-Q, Yu Y-H, Xu L. Preparation, physicochemical and functional characterization of pectic polysaccharides from fresh passion fruit peel by magnetic-induced electric field-assisted three-phase partitioning. Food Hydrocoll. 2024;156:110292. https://doi.org/10.1016/j.foodhyd.2024.110292.
46. Ramos BP, Perez ID, Wessling M, Boina RF. Metal recovery from multi-elementary electroplating wastewater using passion fruit powder. J Sustain Metall. 2021;7(3):1091-101. https://doi.org/10.1007/s40831-021-00398-4.
47. Manyangadze M, Chikuruwo NHM, Narsaiah TB, Chakra CS, Radhakumari M, Danha G. Enhancing adsorption capacity of nano-adsorbents via surface modification: a review. S Afr J Chem Eng. 2020;31:25-32. https://doi.org/10.1016/j.sajce.2019.11.003.
48. Droste RL. Theory and practice of water and wastewater treatment. Hoboken: John Wiley & Sons; 2018.
49. Yurtsever M, Sengil ÌA. Biosorption of Pb(II) ions by modified quebracho tannin resin. J Hazard Mater. 2009;163(1):58-64. https://doi.org/10.1016/j.jhazmat.2008.06.077. PMid:18667272.
50. Lima EC, Royer B, Vaghetti JCP, Simon NM, Da Cunha BM, Pavan FA, et al. Application of Brazilian pine-fruit shell as a biosorbent to removal of reactive red 194 textile dye from aqueous solution: kinetics and equilibrium study. J Hazard Mater. 2008;155(3):536-50. https://doi.org/10.1016/j.jhazmat.2007.11.101. PMid:18178307.
51. Pavan FA, Camacho ES, Lima EC, Dotto GL, Branco VTA, Dias SLP. Formosa papaya seed powder (FPSP): Preparation, characterization and application as an alternative adsorbent for the removal of crystal violet from aqueous phase. J Environ Chem Eng. 2014;2(1):230-8. https://doi.org/10.1016/j.jece.2013.12.017.
52. Coelho GF, Gonçalves AC Jr, Tarley CRT, Casarin J, Nacke H, Franciskowski MA. Removal of metal ions Cd (II), Pb (II), and Cr (III) from water by the cashew nut shell Anacardium occidentale L. Ecol Eng. 2014;73:514-25. https://doi.org/10.1016/j.ecoleng.2014.09.103.
53. Honorato AC. Biossorção do corante azul reativo 5G em efluentes têxteis utilizando resíduos agroindustriais. [dissertação]. Toledo: Universidade Estadual do Oeste do Paraná; 2015 [cited 2025 Feb 5]. Available from: https://tede.unioeste.br/handle/tede/1819
54. Hamidi A, Yeddou-Mezenner N, Lounis A. Eco-Friendly scolymus hispanicus for the Removal of Basic Blue 41. Iran J Chem Chem Eng. 2021;40(2):511-23.
55. Marin P, Borba CE, Módenes AN, De Oliveira SPD, Figueiredo LS, Passaia N. Avaliação do efeito da temperatura, pH e granulometria do adsorvente na adsorção do corante azul reativo 5G. Engevista. 2015;17(1):59. https://doi.org/10.22409/engevista.v17i1.542.
56. Shrivastava P, Dwivedi MK, Malviya V, Jain P, Yadav A, Jain N. Adsorption of Crystal violet dye from aqueous solution by activated sewage treatment plant sludge. Desalination Water Treat. 2023;283:222-36. https://doi.org/10.5004/dwt.2023.29210.
57. Youssef HM, Guesmi A, Hamadi NB, Alotaibi MT, El-Sayed M, Mubarak MF. Aluminum foam-based sandwich composites for high-efficiency removal of reactive blue 19 dye. J Indian Chem Soc. 2026;103(2):102403. https://doi.org/10.1016/j.jics.2026.102403.
58. Honda MDH, Borthakur D. Low pKa values of acid hydrogen donor groups in mimosine enable efficient iron chelation at alkaline pH. J Mol Struct. 2026;1353:144769. https://doi.org/10.1016/j.molstruc.2025.144769.
59. Penha AVS, Moura KO, Paz GL. Tratamento de águas residuais: uma revisão sobre a adsorção do corante preto de amido 10B. Rev Virtual de Quím. 2021;13(2):581-92. https://doi.org/10.21577/1984-6835.20210010.
60. Long J, Yuvaraja G, Zhou S, Mo J, Li H, Luo D, et al. Inactive Fusarium Fungal strains (ZSY and MJY) isolation and application for the removal of Pb(II) ions from aqueous environment. J Ind Eng Chem. 2019;72:442-52. https://doi.org/10.1016/j.jiec.2018.12.047.
61. Ezeh K, Ogbu IC, Akpomie KG, Ojukwu NC, Ibe JC. Utilizing the sorption capacity of local Nigerian Sawdust for attenuation of heavy metals from solution: isotherm, kinetic and thermodynamic investigations. Pac J Sci Technol. 2017;18(1):251-64.
62. Bezerra PQM, De Matos MFR, Ramos IG, Magalhães-Guedes KT, Druzian JI, Costa JAV, et al. Innovative functional nanodispersion: combination of carotenoid from Spirulina and yellow passion fruit albedo. Food Chem. 2019;285:397-405. https://doi.org/10.1016/j.foodchem.2019.01.181. PMid:30797363.
63. Abidi N, Cabrales L, Haigler CH. Changes in the cell wall and cellulose content of developing cotton fibers investigated by FTIR spectroscopy. Carbohydr Polym. 2014;100:9-16. https://doi.org/10.1016/j.carbpol.2013.01.074. PMid:24188832.
64. Habib MA, Maheswari SP. Electrochromism of polyaniline: an in situ FTIR study. J Electrochem Soc. 1989;136(4):1050-3. https://doi.org/10.1149/1.2096782.